

Effect of Temperature on Mn²⁺ Doped LiPbX₃ (X = Cl, Br, I): Synthesis and Characterization

A. J. Nadgowda, S. B Pandey, C. S Khade

Department of Physics, G. H. Rasoni University, India

Abstract: In this current paper, the molar feed ratio of MnCl₂ to PbBr₂ is 1.35 M%. Lead halide perovskite is synthesized by the wet chemical method. The structure of LiPb(Cl/Br)₃ doped with Mn²⁺ nanocrystal was confirmed by TEM analysis and XRD with JCPDS#73-0692. All the diffraction peaks slightly shifted towards the lower angle, this may be due to cell size increases after the Br ion is included in the LiPb(Cl/Br)₃ nanocrystal. The cause of the dual color emission of the LiPb(Cl/Br)₃ doped with Mn²⁺ nanocrystal when excited with a 365 nm UV lamp is a transfer of energy levels between the 4T₁ and 6A₁ of the Mn²⁺ 3d state (d-d) transition. With increasing the temperature of synthesis under 365 nm UV excitation, a red shift is observed from 598 nm to 605 nm.

Keywords: perovskites.

1. Introduction

Because perovskites are widely utilized in solar cells and other optoelectronic devices, their unique physical, electrical, and photoluminescent features have garnered significant attention in the research community nowadays. Perovskites with halide-based phosphors are commonly used in photovoltaic and optoelectronic applications because of their excellent light-absorbing capabilities. [1] The first photovoltaic device based on halide-perovskite (CH₃NH₃PbI₃) attained a 3.8% power conversion efficiency. Kojima and associates. [2] It increased even more to 22.1%, sparking the curiosity of experts. Halide perovskites are useful because of their chemical tenability in many optoelectronic devices. These include devices that produce light through stimulated radiation emission, such as lasers, transistors, spintronics, and light-emitting electrochemical cells (LECs). [3] Due to the benefits they offer, perovskites have been a popular choice for solar cell material. These characteristics include a maximum absorption coefficient, an adjustable electronic energy band gap (E_g) in the solar photon energy spectrum, inexpensive solution processing costs, and more. [4-6]. Despite the great power conversion efficiency of lead-based perovskites, lead toxicity restricts their wider commercialization. [7-8]. Even though many other kinds of solar cells have been created, perovskite-based solar cells could be the solar cells of the future.

Recently, there has been a lot of interest in solution-processed mixed and inorganic lead halide perovskites due to their potential features in photophysical applications such as LEDs, lasers, and photodetectors.[9-13] These perovskites feature high PLQY, small exciton binding energy, and a balanced electron and hole mobility lifetime. Because of their extreme vulnerability to oxygen and moisture, however, the mixed lead halide perovskites have only limited practical applications. Inorganic lithium lead halide (LiPbX₃, X = Cl, Br, and I) nanocrystals are substantially more stable than their organic-inorganic perovskite counterparts. Additionally, the LiPbX₃ perovskite nanocrystals have considerable potential in optoelectronic applications because of their excellent photoluminescence quantum yields without any extra

surface passivation and because they can have their optical characteristics tuned across the whole visible spectrum.[14-15]

2. Synthesis Process

Wet chemical synthesis methods are commonly used for the preparation of perovskite materials [16-17] like LiPbX₃ (where X = Cl, Br, I). Here, we follow a general procedure for the wet chemical synthesis of LiPbX₃ compounds using lithium halide (LiX) and lead halide (PbX₂) as starting materials. We weigh the appropriate amounts of lithium halide (LiX) and lead halide (PbX₂) according to the desired stoichiometric ratio. Ensure precision in measurements for accurate results. Then we dissolve lithium halide (LiX) in a suitable solvent (e.g., DMF, DMSO) to create a lithium halide solution. Stir the solution until the LiX is completely dissolved. Similarly, dissolve lead halide (PbX₂) in the same or a separate container using the same solvent to create a lead halide solution. We stirred this solution until the PbX₂ was fully dissolved. Then we combine the lithium halide solution and the lead halide solution in the desired stoichiometric ratio (1:1 for LiPbX₃) in a reaction vessel (e.g., a flask or beaker). Stir the mixture thoroughly to ensure homogeneity.

As we mix the solutions, a white or yellow precipitate of LiPbX₃ starts to form. This is the desired perovskite product. Once the precipitation is complete, we separate the solid LiPbX₃ product from the solution using vacuum filtration or gravity filtration with filter paper. We wash the collected solid product with a suitable solvent (e.g., ethanol or acetone) to remove impurities and any unreacted starting materials. Wash until the filtrate is clear.

Transfer the washed LiPbX₃ precipitate to a clean container and allow it to air dry or place it in an oven at a low temperature (e.g., 50-80°C) to ensure complete drying. This step is essential to removing any remaining solvent. Characterize the obtained LiPbX₃ compound using analytical techniques such as X-ray diffraction (XRD), Fourier-transform infrared spectroscopy (FTIR), and scanning electron microscopy (SEM) to confirm its composition, structure, and purity.

3. Results and Discussion

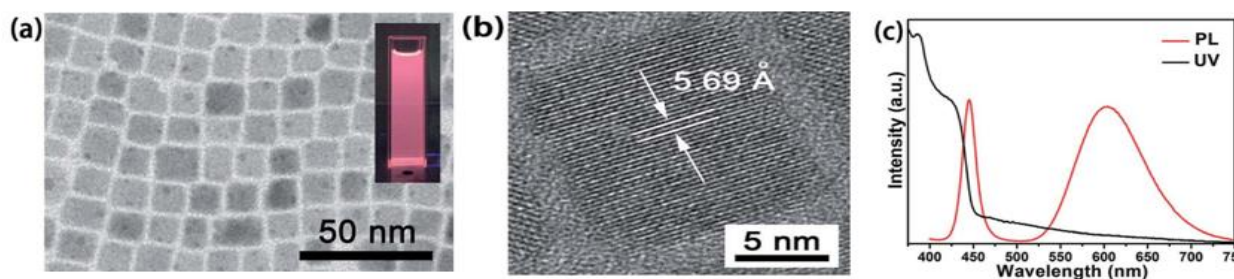


Figure 1.1 TEM image (a), HRTEM image (b), absorption spectra (c)

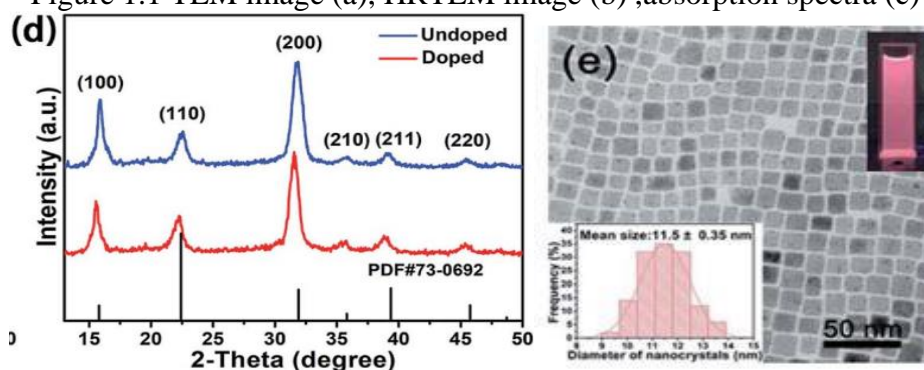


Figure 1.2 PL emission spectra excited by 365 nm UV light (c) and XRD pattern of Mn-doped LiPb(Cl/Br)₃ NCs (d), TEM image for MnCl₂ to PbBr₂ for 1.35 M%.

For preparation of $\text{LiPb}(\text{Cl}/\text{Br})_3$ nano crystals doped with Mn^{2+} , MnCl_2 is added to PbBr_2 precursors in a colloidal solution. The water is evaporated from a combination of ammonia, and ODE at 120°C while the molar feed ratio of MnCl_2 and PbBr_2 is 1.35. After that, it's crucial to heat everything up over 200°C to fully dissolve the metal salts. To get the Mn-doped $\text{LiPb}(\text{Cl}/\text{Br})_3$ NCs, the temperature is lowered to 180°C , cool the compound at room temperature and wash it again with acetone. Put it in oven at 50°C to 80°C till it completely dry. Crushed the prepared material and used it for further characterization. Nanostructures of Mn-doped $\text{LiPb}(\text{Cl}/\text{Br})_3$ NCs were obtained by transmission electron microscopy (TEM) after their preparation. TEM analysis of as-prepared Mn-doped $\text{LiPb}(\text{Cl}/\text{Br})_3$ NCs shows as shown in fig. 1.1(e) that they are cubic in shape and average 11.5 nm in size. Figure 1.1 (d) shows the Mn-doped $\text{LiPb}(\text{Cl}/\text{Br})_3$ NCs' phase structure with the help of X-ray diffraction (XRD) In comparison to undoped cubic LiPbCl_3 nanocrystals (space group $\text{Pm}\bar{3}\text{m}$, PDF#73-0692), all of the diffraction peaks of Mn-doped $\text{LiPb}(\text{Cl}/\text{Br})_3$ NCs shifted slightly to lower angles. This may be because the cell size increases after Br ion mixed into LiPbCl_3 NCs, causing all the peaks to shift to lower angles. In addition, the XRD results shows that the as-prepared nano crystal $\text{LiPb}(\text{Cl}/\text{Br})_3$ doped with have the same cubic phase structure as the undoped LiPbCl_3 NCs, which suggest that the rigidity of the cationic framework of the perovskite prevents any changes to the crystal structure during the doping process. From fig. 1.1 (b) (HRTEM) picture shows that, the interplanar spacing of its (100) plane set is 5.69 \AA , which is bigger than the 5.6 \AA of LiPbCl_3 . This also shows that the Mn doped NC in its as-prepared form has $\text{LiPb}(\text{Cl}/\text{Br})_3$ as its host. High crystalline nature of Mn doped $\text{LiPb}(\text{Cl}/\text{Br})_3$ NCs is reflected by broad XRD peaks and a HRTEM picture. [18-19]

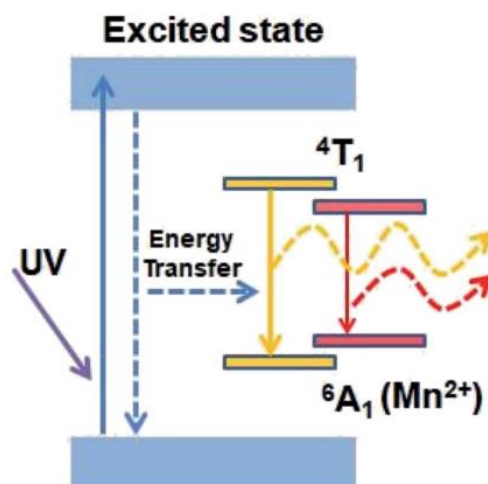


Figure 1.3 Energy levels and fluorescent mechanism of Mn-doped $\text{LiPb}(\text{Cl}/\text{Br})_3$ NCs.

Figure 1.1 © indicates the UV-vis absorption and photoluminescence spectra of $\text{LiPb}(\text{Cl}/\text{Br})_3$ NCs doped with Mn dispersed in cyclohexane allowed us to learn more about their optical characteristics after synthesis. Same figure shows the photoluminescence emission spectra of Mn-doped $\text{LiPb}(\text{Cl}/\text{Br})_3$ NCs synthesis at constant molar feed ratio MnCl_2 to PbBr_2 is equal to 1.35M% but varying the synthesis temperature. When excited to UV radiation at 365 nm wavelength two different peaks was observed one at 445 nm which represents the host material $\text{LiPb}(\text{Cl}/\text{Br})_3$ and the other at 600 nm when Mn^{2+} is doped into host synthesis at 160°C , 180°C , and 200°C . Dual-color emissions are clearly visible in the PL spectrum. This wide emission at 600 nm, due to transfer of energy between ${}^4\text{T}_1$ & ${}^6\text{A}_1$ levels of Mn^{2+} 3d state as shown in figure 1.3.

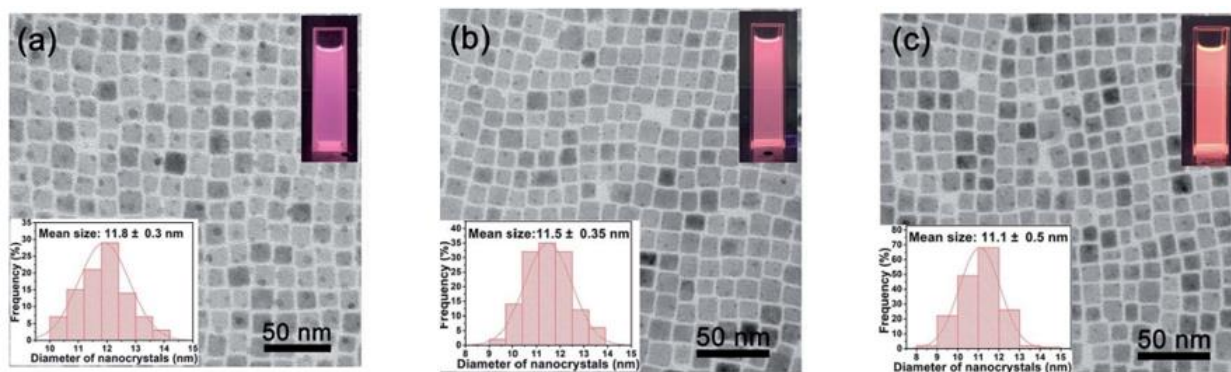


Figure 1.4 Transmission electron microscope (TEM) images of $\text{LiPb}(\text{Cl}/\text{Br})_3$ doped with the Mn, NCs prepared at different synthesis temperature: (a) 160°C , (b) 180°C , (c) 200°C but at constant molar feed ratio 1.35M%

TEM pictures of $\text{LiPb}(\text{Cl}/\text{Br})_3$ doped with Mn NCs generated at various temperatures but with a constant molar feed ratio of 1.35M% are shown in Fig. 1.4 These results indicates that the particle size does not affected by synthesis temperature. The TEM image diagram displays the associated particle size distribution and the PL pictures of the cyclohexane nanocrystal solution when exposed to 365 nm UV light.

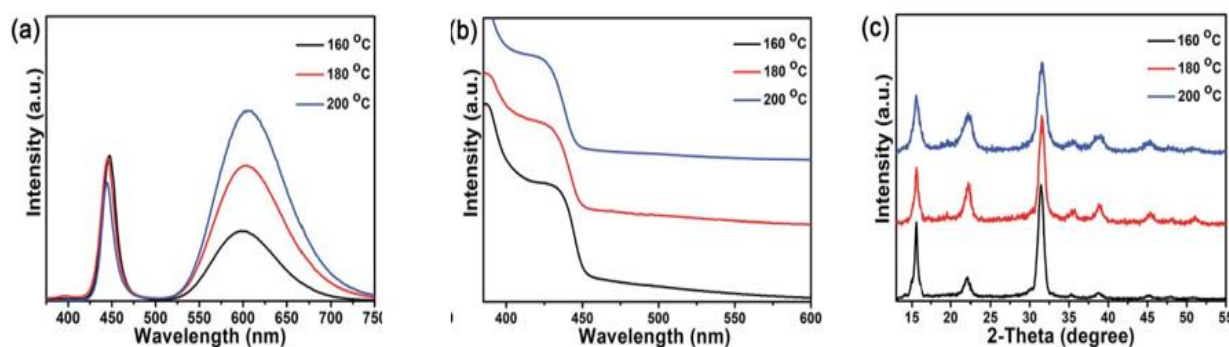


Figure 1.5 (a) Photoluminescence emission spectra (b) emission spectra of the Mn-doped $\text{LiPb}(\text{Cl}/\text{Br})_3$ NCs that are prepared at 160, 180 and 200 C with the MnCl_2 -to- PbBr_2 molar feed ratio of 1.35 & (c) XRD

From fig. 1.5 (a) we can say that the host material $\text{LiPb}(\text{Cl}/\text{Br})_3$ gives a emission peak at 445 nm and when Mn^{2+} doped into host material a wide emission from 598 nm to 605 nm is observed at different synthesis temperature. From above we can say that as synthesis temperature increases from 160°C to 200°C the emission spectra shift from 598nm to 605 nm, this may be because higher proportion on Mn results in a greater number of Mn to Mn couple being formed Crystalline cubic LiPbCl_3 is maintained in Mn-doped $\text{LiPb}(\text{Cl}/\text{Br})_3$ NCs generated at varying reaction temperatures. There are virtually any discernible changes to the diffraction peaks throughout this procedure since the Mn^{2+} substitution ratio does not rise obviously.

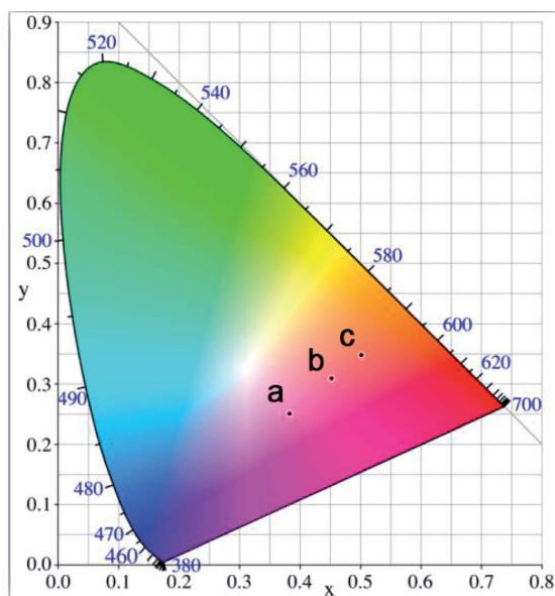


Figure 1.6 CIE chromaticity diagram of the Mn-doped $\text{LiPb}(\text{Cl}/\text{Br})_3$ NCs prepared at different reaction temperature: (a) 160 C, (b) 180 C, (c) 200 C.

Finally, CIE chromaticity coordinates were derived and shown in Fig. 1.6 to assess the impact of reaction temperature on luminous emission colour. UV light at 365 nm excites nanocrystals in a cyclohexane solution, and the resulting photoluminescence (PL) pictures are shown above (Fig. 1.5 (a)). The optical characteristics of Mn-doped $\text{LiPb}(\text{Cl}/\text{Br})_3$ NCs are affected by both the molar feed ratio of MnCl_2 to PbBr_2 and the reaction temperature.

4. Conclusion:

In conclusion, we present paper host $\text{LiPb}(\text{Cl}/\text{Br})_3$ NCs and Mn^{2+} is used as a dopant for molar feed ration of MnCl_2 -to- PbBr_2 is 1.35 M% synthesis temperature 180°C the crystal structure is confirmed by XRD (PDF#73-0693) and TEM analysis shows that compound was manufactured with particle size 11.5 nm fig.1.1(d). In PL emission two different peaks was observed for host at 445 nm and when Mn^{2+} doped 598 to 605 nm, a wide emission that may be due to transition between ${}^4\text{T}_1$ & ${}^6\text{A}_1$ energy levels of Mn^{2+} 3d state as shown in figure 1. From fig 1.5(a) we conclude that synthesis temperature does not affect the Photoluminescence characteristics of Mn-doped $\text{LiPb}(\text{Cl}/\text{Br})_3$ NCs . CIE diagram shows that Mn-doped $\text{LiPb}(\text{Cl}/\text{Br})_3$ NCs may be used for optoelectronics devices, LCD etc.

References

- [1] Jiabao Li a b, Jialong Duan a, Xiya Yang a, Yanyan Duan c, Peizhi Yang b, Qunwei Tang a Review on recent progress of lead-free halide perovskites in optoelectronic applications, Volume 80, February 2021, 105526
- [2] Jiang Liu a, Jiahui Lin a, Qifan Xue b, Qinyan Ye a, Xulin He a, Liangqi Ouyang c, Daming Zhuang c, Cheng Liao a, Hin-Lap Yip b, Jun Mei a, Woon-Ming Lau a Growth and evolution of solution-processed $\text{CH}_3\text{NH}_3\text{PbI}_3\text{-xCl}_x$ layer for highly efficient planar-heterojunction perovskite solar cells, Volume 301, 1 January 2016, Pages 242-250
- [3] He Dong, Chenxin Ran, Weiyin Gao, Mingjie Li, Yingdong Xia & Wei Huang , Metal Halide Perovskite for next-generation optoelectronics: progresses and prospects, volume 3, Article number: 3 (2023)

- [4] Minghao Wang, Wei Wang, Ben Ma, Wei Shen, Lihui Liu, Kun Cao, Shufen Chen & Wei Huang Lead-Free Perovskite Materials for Solar Cells, volume 13, article number 62,(2021)
- [5] Kumar Elangovan a, Raju Kannadasan a, B.B. Beenarani b, Mohammed H. Alsharif c, Mun-Kyeom Kim d, Z. Hasan Inamul e Recent developments in perovskite materials, fabrication techniques, band gap engineering, and the stability of perovskite solar cells, Volume 11, June 2024, Pages 1171-1190
- [6] Ibrahim, Amar Shoukat, Fawad Aslam, &M. Israr Ur Rehman, Emerging trends in low band gap perovskite solar cells: materials, device architectures, and performance optimization, Article: e2316273 | Received 08 Dec 2023, Accepted 04 Feb 2024, Published online: 14 Feb 2024
- [7] Abhishek Srivastava a, Jena Akash Kumar Satrughna b, Manish Kumar Tiwari a, Archana Kanwade a, Subhash Chand Yadav a, Kiran Bala c, Parasharam M. Shirage a , Lead metal halide perovskite solar cells: Fabrication, advancement strategies, alternatives, and future perspectives, Volume 35, June 2023, 105686
- [8] IRui Wang 1 5, Jintao Wang 2 5, Shaun Tan 1, Yu Duan 1 2, Zhao-Kui Wang 1 3, Yang Yang 1 4 , Opportunities and Challenges of Lead-Free Perovskite Optoelectronic Devices, Volume 1, Issue 4, July 2019, Pages 368-379
- [9] Lixiu Zhang, Luyao Mei, Advances in the Application of Perovskite Materials, Volume 15, article number 177, (2023)
- [10] Jianping Deng, All-inorganic Lead Halide Perovskites: A Promising Choice for Photovoltaics and Detectors , Journal of Materials Chemistry C 7(40), September 2019,7(40)
- [11] Amrita Dey, Junzhi Ye, Apurba De, State of the Art and Prospects for Halide Perovskite Nanocrystals, ACS Nano 2021, 15, 7, 10775–10981
- [12] Qi Chen a b, Nicholas De Marco a b, Under the spotlight: The organic–inorganic hybrid halide perovskite for optoelectronic applications, Volume 10, Issue 3, June 2015, Pages 355-396.
- [13] Chandrasekar Perumal Veeramalai, Shuai Feng, Lead–halide perovskites for next-generation self-powered photodetectors: a comprehensive review, Photonics Research, Vol. 9, Issue 6, pp. 968-991(2021)
- [14] V. G. Vasavi Dutt,a Syed Akhila Enhancement of photoluminescence and the stability of CsPbX₃ (X = Cl, Br, and I) perovskite nanocrystals with phthalimide passivation ,Nanoscale, Issue 34 (2021)
- [15] Andrés F. Gualdrón-Reyes, Progress in halide-perovskite nanocrystals with near-unity photoluminescence quantum yield, Trends in Chemistry 3(6), April 2021, 3(6)
- [16] Dinesh Kumar, Ram Sagar Yadav, Monika, Akhilesh Kumar Singh and Shyam Bahadur Rai, Synthesis Techniques and Applications of Perovskite Materials , Submitted: 12 March 2019 Reviewed: 13 May 2019 Published: 10 June 2020
- [17] Nada F. Atta, Ahmed Galal and Ekram H. El-Ads, Perovskite Nanomaterials – Synthesis, Characterization, and Applications , Submitted: 31 March 2015 Reviewed: 18 August 2015 Published: 03 February 2016
- [18] Pengchao Wang, Bohua Dong, Zhenjie Cui, Rongjie Gao, Ge Su, Wei Wang, and Lixin Cao , Synthesis and characterization of Mn-doped CsPb(Cl/Br)₃ perovskite nanocrystals with controllable dual-color emission, RSC Adv. 2018 Jan 5; 8(4): 1940–1947.
- [19] Pengchao Wang, Synthesis and characterization of Mn-doped CsPb(Cl/Br)₃ perovskite nanocrystals with controllable dual-color emission , January 2018,8(4):1940-1947